International Journal of Nuclear Security

Volume 8 | Number 1 Article 10

12-2023

Tests of a Gamma Spectrometer-Neutron Counter Relationship as a Neutron Alarm Metric in Mobile Radiation Search Systems

Jackson N. Wagner
Texas A&M University

Craig Marianno
Texas A&M University

Recommended Citation
Wagner, Jackson N. and Marianno, Craig (2023) "Tests of a Gamma Spectrometer-Neutron Counter Relationship as a Neutron Alarm Metric in Mobile Radiation Search Systems," *International Journal of Nuclear Security*: Vol. 8: No. 1, Article 10.
https://doi.org/10.7290/ijns08497795
Available at: https://trace.tennessee.edu/ijns/vol8/iss1/10

Tests of a Gamma Spectrometer-Neutron Counter Relationship as a Neutron Alarm Metric in Mobile Radiation Search Systems

Cover Page Footnote

The authors wish to thank Kevin G. Hart of Sandia National Laboratories and of the US Department of Energy's Radiological Assistance Program for providing portions of the data analyzed for this work.

International Journal of Nuclear Security, Vol. 8, No. 1, 2023

Tests of a Gamma Spectrometer–Neutron Counter Relationship as a Neutron Alarm Metric in Mobile Radiation Search Systems

Jackson Wagner and Craig Marianno
Texas A&M University

Abstract

A mobile radiological search system (MRSS) is frequently used in nuclear security to interdict illicit nuclear material. One difficulty an MRSS faces is in characterizing its detectors' background responses, particularly in its neutron counter(s). This difficulty adds complications to identifying the presence of neutron-emitting radiological materials during an operation. Fortunately, previous work has identified a power law relationship between muons registered by the MRSS's gamma detectors and background neutrons. This relationship can be applied to estimate the MRSS's background neutron count rate using that muon count rate. To test the usability of such an estimate, an MRSS was used to sweep a parking garage that had an 886 kBq ^{252}Cf source present on various levels. A moving average of the MRSS's muon count rate was used to estimate the background neutron count rate, and that dynamic estimate was compared against the observed neutron count rate to determine whether an alarm should occur. For a "control" method, a similar comparison was made between the observed neutron count rate and a constant estimate of the neutron background, where the latter came from a 6-minute measurement of the neutron background outside the parking garage. The results showed that the dynamic estimate of the neutron background performed as well as the constant estimate when identifying whether the ^{252}Cf was present, particularly when the MRSS was on the same level as the material. In many cases, the dynamic estimate produced stronger evidence in favor of an alarm than the constant estimate, and the dynamic estimate was also more likely to produce an alarm when the MRSS was on a level adjacent to the ^{252}Cf. In addition to these results, the dynamic method appeared to have similar performance as the constant method when outside the parking garage. All of these data indicates that applying the neutron–muon power law relationship improves an MRSS's sensitivity to manmade neutron sources in extreme

DOI: 10.7290/ijns08497795

International Journal of Nuclear Security, Vol. 8, No. 1, 2023

environments (such as a parking garage or urban center) while maintaining its sensitivity in more normal, open environments.

Keywords: neutron detection, gamma scintillation, nuclear security, mobile search, neutron counting, neutron alarm, neutron background, muon background

1. Introduction

Nuclear security operators frequently employ mobile radiation search systems (MRSSs) to screen areas for illicit nuclear materials. These vehicle-mounted systems can be employed for operations that require securing an area either before a major public event (such as a sporting event or presidential inauguration) or during an incident response (where such devices may have already been used). Fortunately, radiological material emits characteristic radiation, specifically gamma rays and neutrons, and an MRSS thus employs gamma spectroscopy and neutron counting radiation detectors to aid in locating these materials.

One requirement in these operations is understanding the ambient (or *background*) detector response, which is necessary for them to alarm when in the presence of artificial radioactive material. This response is essential because all alarms require adjudication, including incorrect ones, and the adjudication of these false alarms results in time lost during these extremely time-sensitive operations. Unfortunately, the fact that these systems are always moving makes characterizing much more difficult than what would be needed for stationary laboratory measurements. This problem is mitigated in the gamma spectroscopy system because the background produces an energy spectrum that is unique from any artificial materials. Conversely, the neutron counting system does not have such a unique background response, and complexities in neutron physics cause that response to be affected in more ways than would occur in the gamma spectrometer.

Fortunately, previous research has shown that the problems with characterizing the neutron background can be mitigated using data from the gamma spectrometer after small modifications. That work found that when calibrated for much higher energy scales (up to 70 MeV instead of 3–4 MeV), the gamma spectrometer primarily detects muons [1]. These muons are produced by the same processes that produce background neutrons, which suggests that the detection of both particles would vary similarly in background conditions [2]. Further work showed that this detection indeed occurs in these mobile search systems, and the muon and neutron count rates are correlated by a power law relationship [3]. More importantly, no artificial source of muons exists outside of laboratory conditions, which means the muon count rate in a MRSS at any given moment comes from the background. Thus, the power law relationship determined from previous work could conceivably be applied to estimate the background neutron count rate using the muon count rate. That estimate could be used to determine if an artificial neutron source is present.

This research sought to test the applicability of a neutron alarm method derived from the neutron–muon power law relationship derived in previous work, particularly in a

DOI: 10.7290/ijns08497795

International Journal of Nuclear Security, Vol. 8, No. 1, 2023

scenario where the neutron background is expected to change. For this situation, an MRSS's muon count rate was used to estimate its background neutron count rate and compared against what that detector observes when radiological material may be present. A parking garage was selected for these tests because it is the most extreme scenario where the neutron background is likely to change. The development of this method sought to improve the MRSS's capabilities to account for such changes as they would occur in parking garages or urban areas while maintaining its sensitivity to neutron-emitting radiological materials. Because the neutron–muon relationship as it stands is empirical, these tests required the use of the same system as what was used in previous research to develop the relationship [3]. To determine this new method's effectiveness, it was also compared against a more intuitive alarm method from a constant estimate of the neutron count rate.

2. Materials and Methods

As mentioned in the introduction, these tests used the same system as those used to characterize the neutron–muon relationship described in previous work [3]. This research consisted of one 2 × 4 × 16 in. (5.08 × 10.16 × 40.64 cm) NaI detection system with an Ortec digiBASE multichannel analyzer and one Ortec neutron counting system with four 1 × 18 in. (2.54 × 45.72 cm) ^{3}He tubes encased in a high-density polyethylene moderator [4, 5]. The NaI detector's energy calibration was made using ^{137}Cs and ^{22}Na, as shown in Table 1, to achieve an approximately 70 MeV energy scale, and data below channel 62 (of 1024 with the first channel labelled "0") were ignored to discriminate background gamma rays. The energy range of approximately 4 MeV to approximately 70 MeV was used to match the energy range used while characterizing the neutron–muon count rate relationship [3]. The detectors were placed in a vehicle, as shown in Figure 1, with the NaI detector placed lying flat with its largest face parallel to the ground (i.e., with its largest face "looking up" from the vehicle). Data were also collected from a polyvinyl toluene detector in the same orientation and another NaI detector in a different orientation (lying flat with its largest face perpendicular to the ground—"looking out" from the vehicle), but they were not included because their neutron–muon relationships were not as well-defined.

Table 1. Calibration information for the NaI detector.

			^{137}Cs	^{22}Na	
Gamma ray energy		(keV)	662	511	1274
Photopeak	Energy	(keV)	662	511	1274
	Channel number		10.5 ± 1	8 ± 1	19.5 ± 1
Calibration		(keV ch-1)	68.0 ± 10.7		

The parking garage in which these measurements took place was the Central Campus Garage (CCG) on the campus of Texas A&M University. This structure has eight levels of parking space with a mirrored, spiral traffic pattern, where two sides of the same parking level have opposite traffic directions (in terms of moving toward upper or lower levels). Schematics of a selection of the eight levels of CCG are shown in Figure 2. Measurements occurred in "sweeps" of the entire height of the garage. The mobile search system would begin on either the top or bottom level (eight or one, respectively)

DOI: 10.7290/ijns08497795

and follow the normal traffic route as it traversed up and down the garage until the vehicle returned to its starting location.

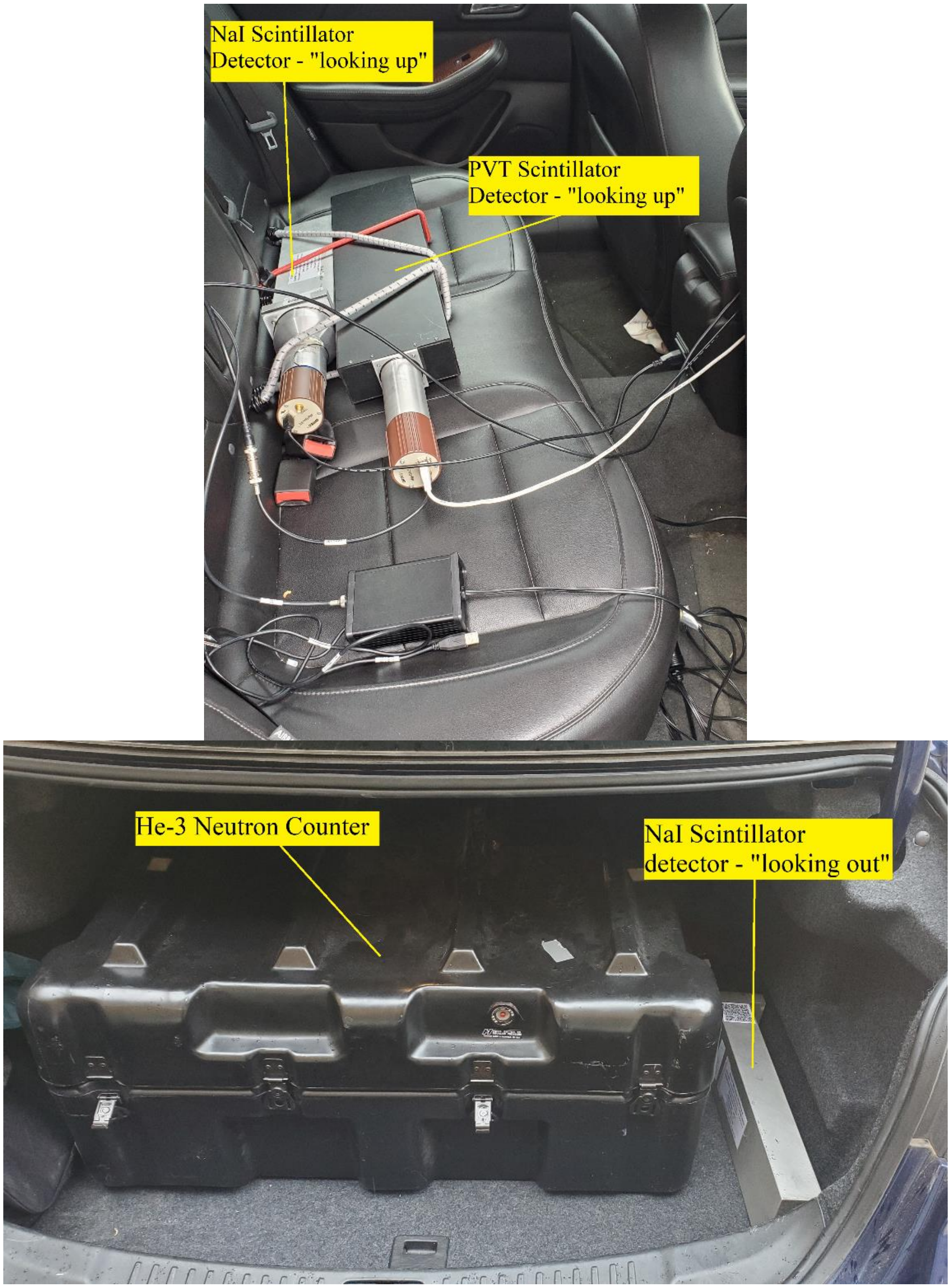

Figure 1. Detector setup in the (top) cabin and (bottom) trunk of a sedan used for mobile search measurements of a parking garage with a neutron source present.

DOI: 10.7290/ijns08497795

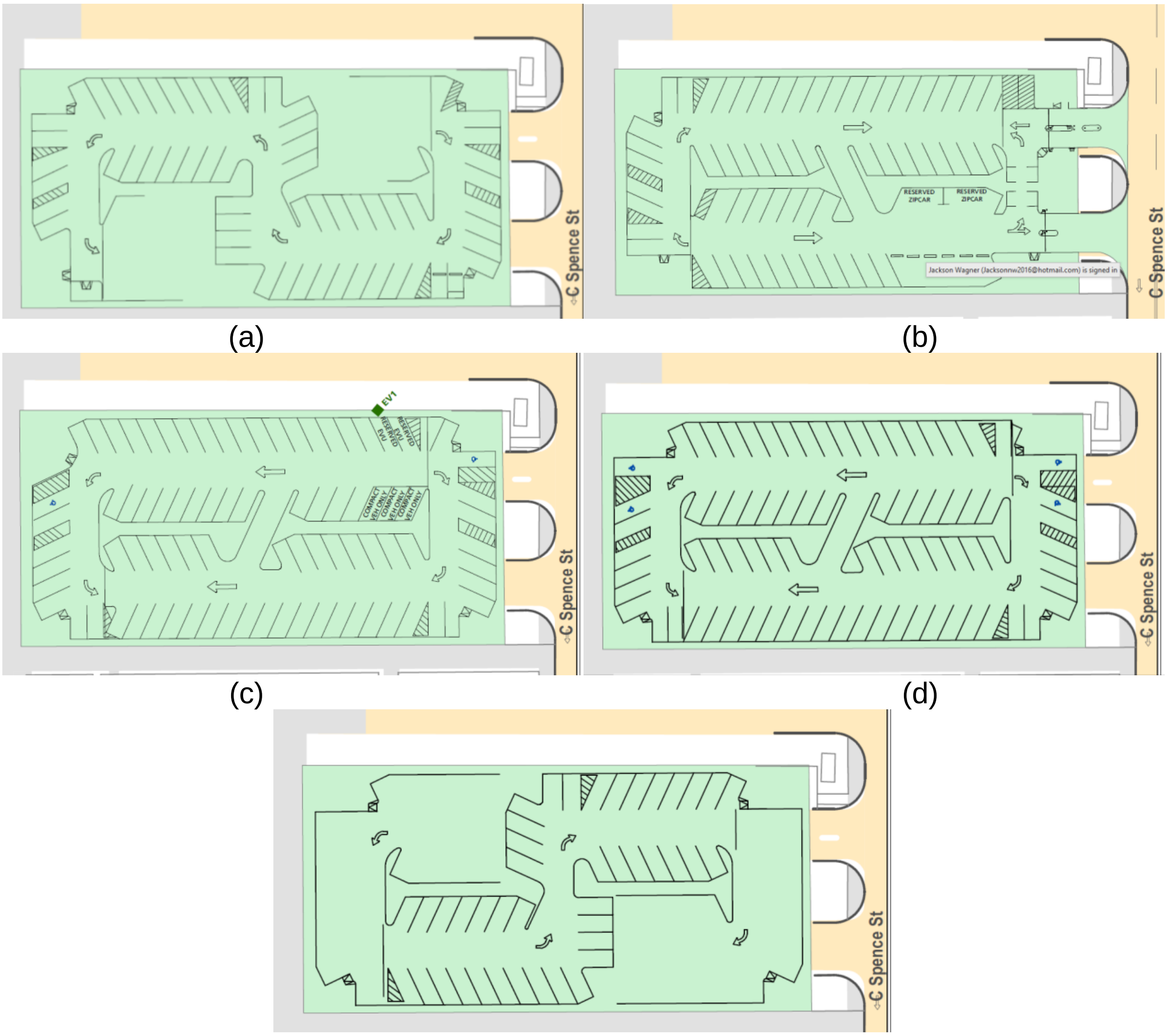

(e)

Figure 2. Maps indicating the layouts and traffic patterns of a selection of levels of CCG, which includes (a) level 1, (b) level 2, (c) level 3, (d) level 7, and (e) level 8. Mobile search sweeps began/ended on either level 1 or 8. During sweeps, the source was placed on the side of a level where traffic travelled downward (the bottom half shown in a, c, and d and the top half shown in b and e).

For each sweep, a ^{252}Cf source was present on one of eight levels of the garage. This source was placed in another vehicle that was parked on a given level on a side where the traffic flow was downward. The ^{252}Cf source had a total activity of approximately 886 kBq and a neutron emission rate of approximately 103,000 s^{-1}. After the eight sweeps with the source, one additional sweep was performed without the source in the garage. All data were collected during a single measurement campaign, and the overall measurement times of that campaign that correlate to the start and end of each sweep are shown in Table 2 with the respective start and source positions. Neutron and muon count rate data collected during these sweeps were used to create two neutron alarm

DOI: 10.7290/ijns08497795

metrics, values which indicate the presence of an artificial neutron source when a certain condition is met.

Table 2. Times in the measurement campaign (in seconds after starting acquisition) that sweeps began and ended, along with the sweep's respective start/end level and source level.

Sweep start/end level	Source level	Start time (s)	End time (s)
1	8	1090	1380
1	7	1450	1725
8	6	1940	2210
8	5	2280	2550
8	4	2630	2900
8	3	3000	3275
8	2	3380	3650
8	1	3770	4040
8	*	4160	4650

*The final background sweep (indicated by Source Level *) consisted of a full sweep that began/ended at level 8, plus a half-sweep as the system returned to level 1 before exiting the garage.

The primary difference between these two metrics is their method for estimating the average neutron count rate. This estimation is essential to an alarm metric, as will be made clear later in this article. The first alarm metric used an intuitive estimation of the average neutron count rate, namely one determined from a brief measurement of known background conditions (i.e., without a neutron source present). In this case, measurements occurred before entering the parking garage while the MRSS was travelling to the area and while it was static nearby (measurements were between 300 s and 700 s relative those shown in Table 2). The estimate of the average neutron count rate then came from the overall average count rate during that period. This average value remained constant and was used throughout measurements, and its alarm metric was used as the control for these tests. The second alarm metric used a calculated estimate of the average neutron count rate based on the neutron–muon relationship defined in previous research. Specifically, the estimated average background neutron count rate was calculated from the measured average muon count rate, as shown in Equation 1 [3]. Unlike the control method, this estimate was dynamic and changed as the muon background changed. These changes occurred frequently in the parking garage with the variances in the amount of concrete shielding, hence its selection as the scenario for these tests.

$$\bar{n} = 0.001149\,\bar{m}^{2.0567}, \tag{1}$$

where $\bar{n}$ is the average neutron count rate (s^{-1}), and $\bar{m}$ is the average muon count rate (s^{-1}).

Using an average value of the neutron and muon count rates was necessary for these alarm metrics because of the characteristics of these particles. The physics that govern the creation and detection of both neutrons and muons result in their measurements

DOI: 10.7290/ijns08497795

being random variables, each with their own probability distribution. Specifically, these are Poisson random variables because measurements of these particles occur by counting the number detected over a given period. This distribution means that the probability of a certain number of counts for each particle within a given time (which are integers greater than or equal to zero) will follow the Poisson probability mass function (pmf), as shown in Equation 2. The shape of a pmf is dictated by its expected counts, λ, within that observation time. Although Equation 2 shows that any observed value (greater than zero) is possible, increasingly large observations relative to the expected value are increasingly unlikely, which is the main aspect for any alarm metric.

$$\mathrm{pmf}(x) = \Pr(X = x) = \frac{\lambda^x}{x!}\mathrm{e}^{-\lambda}, \tag{2}$$

where *X* is the Poisson random variable of counts (integers greater than or equal to zero) observed in a given time with an expected value of λ, *x* is one observation of *X*, Pr(*X* = *x*) is the probability that an observation of *X* will result in x counts, and λ is the expected number of counts from Poisson random variable *X*.

An MRSS would operate under the assumption that no artificial source of neutrons is present (i.e., operators assume it is measuring background), and its alarm algorithm would expect to observe counts within a Poisson distribution that has a known, expected value. In statistics, this assumption would be called the *null hypothesis* and is considered true under most, if not all, scenarios. An alarm occurs when an observation has an exceedingly low probability of occurring as part of the null hypothesis's Poisson distribution, thus providing evidence in favor of an alternative hypothesis. The alternative hypothesis in this case is that an artificial neutron source is present.

Evidence in favor of this alternative hypothesis is indicated when the background Poisson distribution has a low probability of producing a given observation. This probability is calculated by determining the cumulative probability of all count values less than the observation, as described in Equation 3. Because an artificial source of neutrons will increase the expected count rate, larger values from Equation 3 would indicate stronger evidence for rejecting the null hypothesis that counts are from the background. However, the null hypothesis cannot be rejected until the cumulative probability of that value is sufficiently large. This threshold is dictated by the desired maximum probability of false positives (i.e., the likelihood that an incorrect rejection of the null hypothesis might occur). For this research, a false alarm probability of 0.05 was desired because it is what the International Atomic Energy Agency (IAEA) suggests for most measurement operations [6]. This false alarm probability means that the cumulative probability threshold needed to be 0.95. Therefore, if an observation causes Equation 3 to produce a value greater than 0.95, it can be said that the observation likely did not come from background. As a result, the maximum probability of that statement being falsely made would be 0.05 (or 1 in 20, on average).

Although an alarm metric would monitor the result of Equation 3 for values that are greater than 0.95, the asymptotic nature of the Poisson cumulative distribution function makes this difficult to display visually. One solution is to modify the result of Equation 3 by applying the function shown in Equation 4 to generate an alarm metric, M_A. This metric would then be monitored for values that are larger than the threshold dictated by the selected false positive probability, which in this case is $\Pr(X \rightarrow x) = 0.95$ or $M_A = 2.9957$. The value of M_A has no asymptote, which makes its plots as a function of time more visually intuitive, as will be observed later in this article.

$$\Pr(X \rightarrow x) = \Pr(X < x) = \mathrm{e}^{-\lambda} \sum_{i=0}^{x-1} \frac{\lambda^i}{i!} = \mathrm{e}^{-\lambda} \left(1 + \frac{\lambda^1}{1!} + \frac{\lambda^2}{2!} + \cdots + \frac{\lambda^{x-1}}{(x-1)!}\right), \text{and} \quad (3)$$

$$M_{\mathrm{A}} = -\ln(1 - \Pr(X \rightarrow x))\,, \quad (4)$$

where X is the Poisson random variable of counts (integers greater than or equal to zero) observed in a given time with an expected value of λ, x is one observation of X, $\Pr(X \rightarrow x)$ is the probability that observation x is the result of variable X, λ is the expected number of counts from variable X in a given time, and M_A is the alarm metric.

This is not a novel method for calculating an alarm metric and is arguably the simplest method. The main difficulty in its application is in estimating the expected value of λ, the background neutron count rate distribution. Any Poisson random variable's count distribution and its expected value will only match those suggested by Equation 2 with an infinite number of observations, the collection of which is an impossible task for any human. However, any number of observations can produce an estimate of that value, whose accuracy would increase with more observations.

Although an MRSS has significant limitations in the observations it can obtain for its estimate, it still has a variety of techniques to make that estimation. One such technique has already been described: the measurement of the background before entering the garage. The average neutron count rate over this time informed the expected value for the control method's alarm metric. For this work, a background measurement for 400 s prior to entering the garage without a neutron source present yielded an average count rate of approximately 0.17 s^{-1}. As part of the control alarm metric, this average count rate was considered constant; thus, the product of it and the selected observation time of 15 s yielded a constant expected value of approximately 2.6 neutron counts. That expected value was used with observations of neutron counts to calculate values of Equations 3 and 4.

The other estimation technique applied the neutron–muon relationship described in Equation 1. That relationship allowed the estimation to be dynamic, and thus, a much smaller observation time was used to estimate the expected value than that for the control. In this case, the average muon count rate at any given time was calculated using the data from the previous 15 s. That average muon count rate was used in Equation 1 to calculate the average neutron count rate, and—similar to the control method—the expected value was the product of that average neutron count rate and the observation time of 15 s. Although this estimate was dynamic during measurements,

DOI: 10.7290/ijns08497795

it and the observations were used with Equations 3 and 4, whose results were similar to that of the control's estimate.

For both alarm metrics, a constant observation time of 15 s was used throughout the measurements. This value was selected to reduce the random noise that appears in the observations while allowing the data to respond to the variances that occur in the parking garage when traveling at normal speeds. These variances came from the MRSS moving from one level to the next (either up or down), thus changing the amount of nearby shielding, and this process would occur approximately every 20 s during the sweeps. From these data, 15 s was selected to reduce the likelihood that data from the previous level contributed to an observation. From this method, the expected number of neutron counts (or the value of λ in Equation 3) was the product of either method's average value and 15 s. This expected number of counts was then compared against the number of neutron counts measured over the previous 15 s (or the value of x in Equation 3) at any given time. As mentioned previously, a common maximum false positive rate for these systems is 5%. Therefore, an alarm would occur if either method's value for M_A (from Equation 4) was greater than 2.9957, particularly if that condition was met for a sustained period of time.

3. Results and Analysis

Plots of the two alarm metrics' values over time during the measurements are shown in Figures 3 through 10 for sweeps 1 through 8, respectively, as defined in Table 1. These plots include markers showing the times where the sweep started and ended and the time the system reached the garage's *cross-over point*. The times simply indicate when the vehicle started and stopped moving through the garage, and the *cross-over point* means the point where the vehicle reached the top or the bottom of the garage (depending on the level where the sweep started/ended) and thus changed whether it was moving upward or downward.

All these plots show that both methods would have produced alarms when the MRSS was nearest to (or on the same level and side as) the source, as shown by the largest increase in the alarm metric(s). Along with that result, both alarm metrics increased when the system was either on a level adjacent to the source or on the same level as the source but on the opposite side. When that occurred, the metric from the dynamic estimation method of the neutron's expected value was more likely to exceed the alarm threshold and increase more than the constant estimation method.

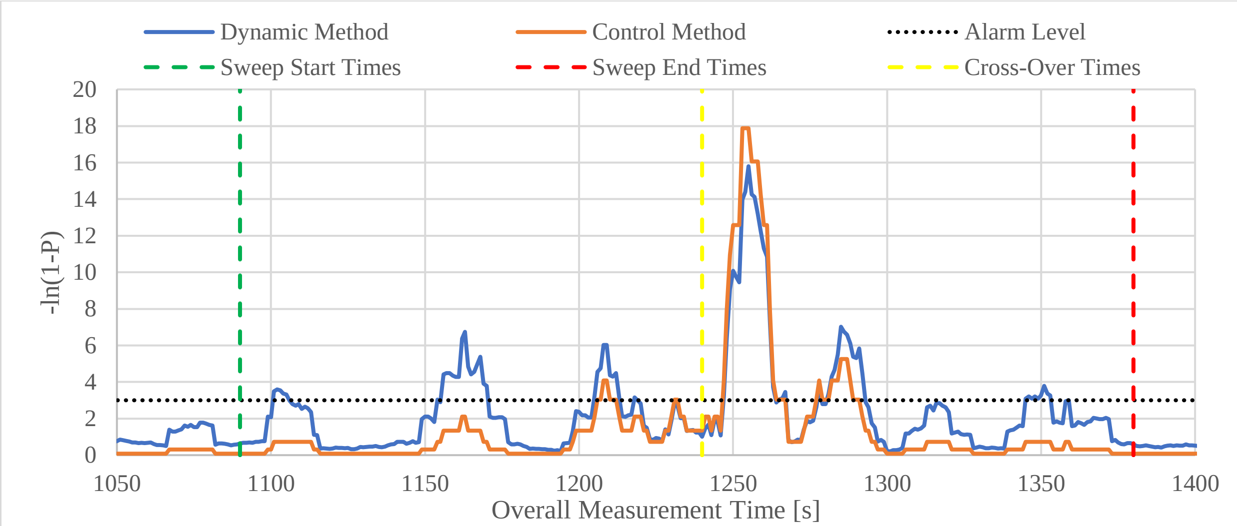

Figure 3. Alarm metrics over time during an MRSS sweep with the source on level 8. The sweep began and ended on level 1, as indicated by the green and red vertical dashed lines, respectively. The yellow vertical dashed line indicates the cross-over point from the upward section of the garage to the downward section on level 8. The dynamic method (blue) calculated the alarm metric using the predicted background neutron count rate, and the control method (orange) calculated the metric using the constant average background neutron count rate. An alarm would occur when these metrics' values were greater than the threshold indicated by the black dotted line.

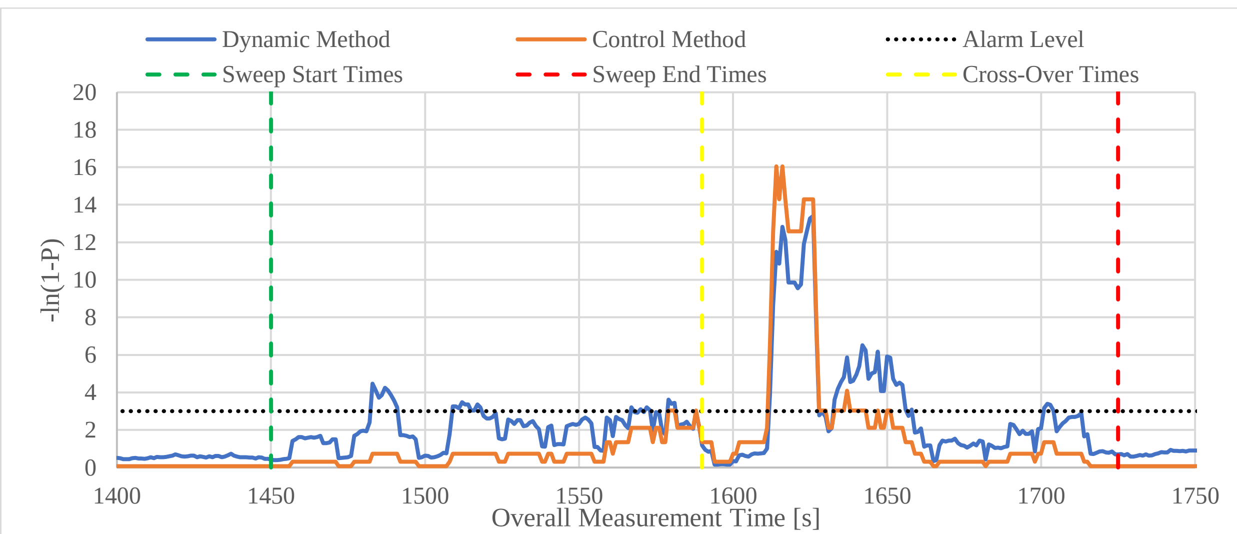

Figure 4. Alarm metrics over time during an MRSS sweep with the source on level 7. The sweep began and ended on level 1, as indicated by the green and red vertical dashed lines, respectively. The yellow vertical dashed line indicates the cross-over point from the upward section of the garage to the downward section on level 8. The dynamic method (blue) calculated the alarm metric using the predicted background neutron count rate, and the control method (orange) calculated the metric using the constant average background neutron count rate. An alarm would occur when these metrics' values were greater than the threshold indicated by the black dotted line.

DOI: 10.7290/ijns08497795

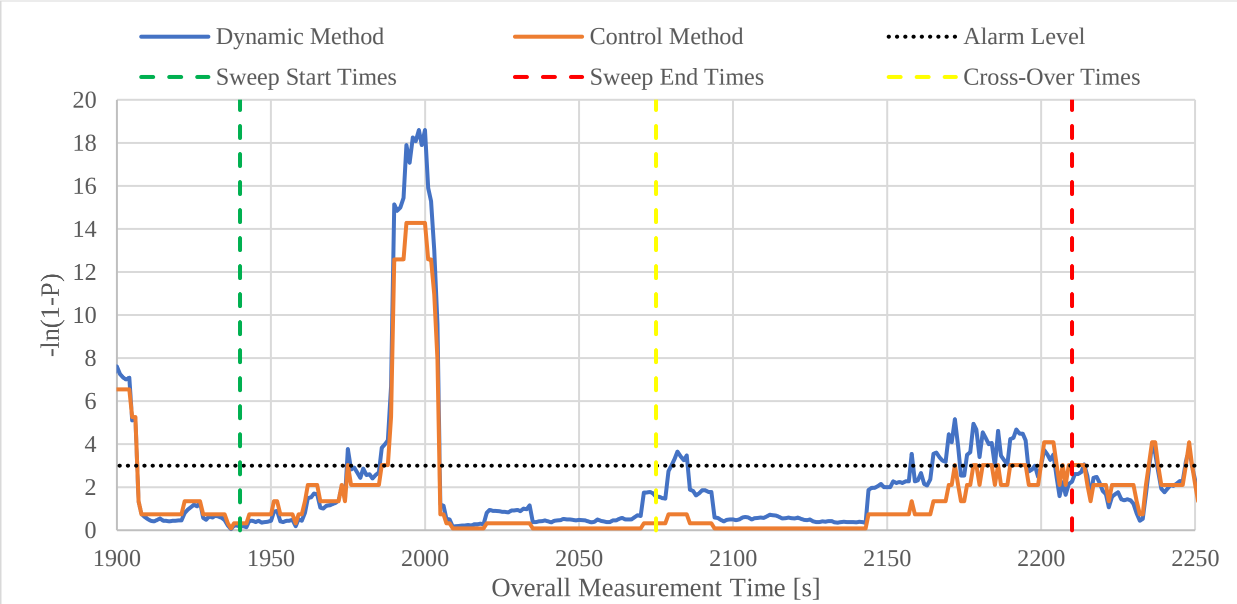

Figure 5. Alarm metrics over time during an MRSS sweep with the source on level 6. The sweep began and ended on level 8 as indicated by the green and red vertical dashed lines, respectively. The yellow vertical dashed line indicates the cross-over point from the downward section of the garage to the upward section on level 1. The dynamic method (blue) calculated the alarm metric using the predicted background neutron count rate, and the control method (orange) calculated the metric using the constant average background neutron count rate. An alarm would occur when these metrics' values were greater than the threshold indicated by the black dotted line.

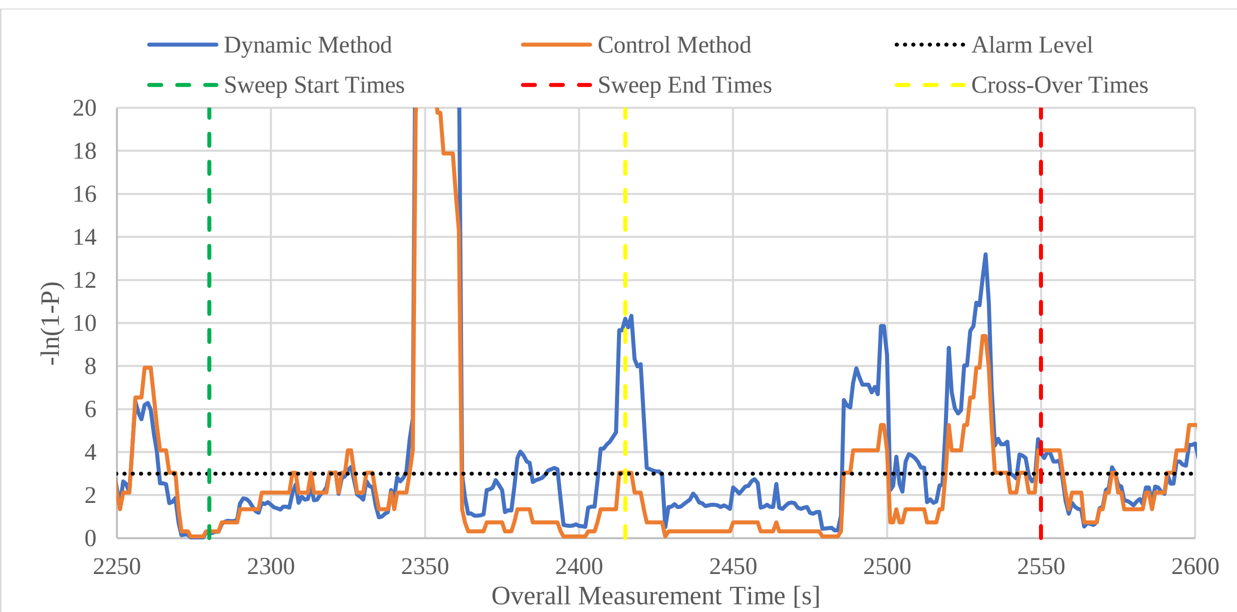

Figure 6. Alarm metrics over time during an MRSS sweep with the source on level 5. The sweep began and ended on level 8, as indicated by the green and red vertical dashed lines, respectively. The yellow vertical dashed line indicates the cross-over point from the downward section of the garage to the upward section on level 1. The dynamic method (blue) calculated the alarm metric using the predicted background neutron count rate, and the control method (orange) calculated the metric using the constant average background neutron count rate. An alarm would occur when these metrics' values were greater than the threshold indicated by the black dotted line.

DOI: 10.7290/ijns08497795

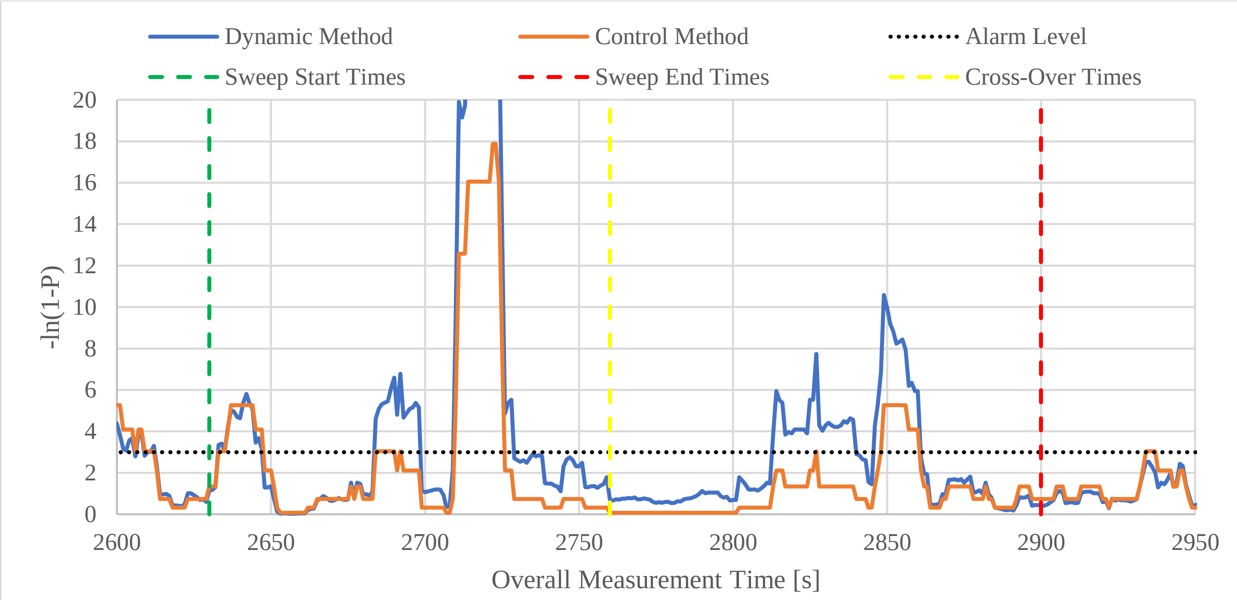

Figure 7. Alarm metrics over time during an MRSS sweep with the source on level 4. The sweep began and ended on level 8, as indicated by the green and red vertical dashed lines, respectively. The yellow vertical dashed line indicates the cross-over point from the downward section of the garage to the upward section on level 1. The dynamic method (blue) calculated the alarm metric using the predicted background neutron count rate, and the control method (orange) calculated the metric using the constant average background neutron count rate. An alarm would occur when these metrics' values were greater than the threshold indicated by the black dotted line.

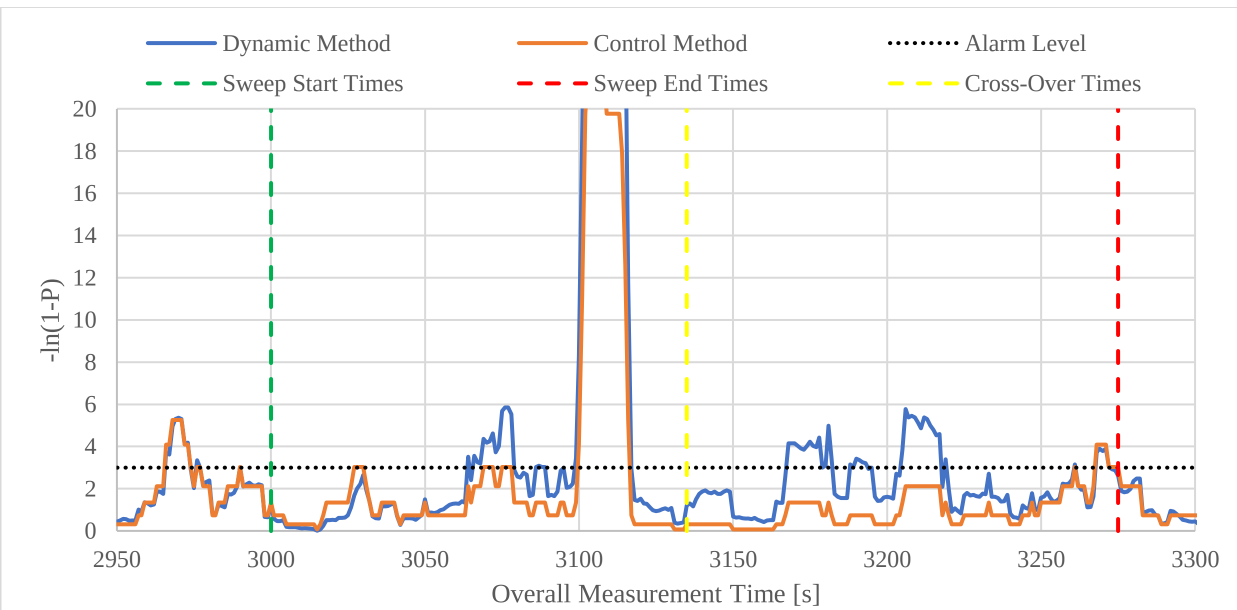

Figure 8. Alarm metrics over time during an MRSS sweep with the source on level 3. The sweep began and ended on level 8, as indicated by the green and red vertical dashed lines, respectively. The yellow vertical dashed line indicates the cross-over point from the downward section of the garage to the upward section on level 1. The dynamic method (blue) calculated the alarm metric using the predicted background neutron count rate, and the control method (orange) calculated the metric using the constant average background neutron count rate. An alarm would occur when these metrics' values were greater than the threshold indicated by the black dotted line.

DOI: 10.7290/ijns08497795

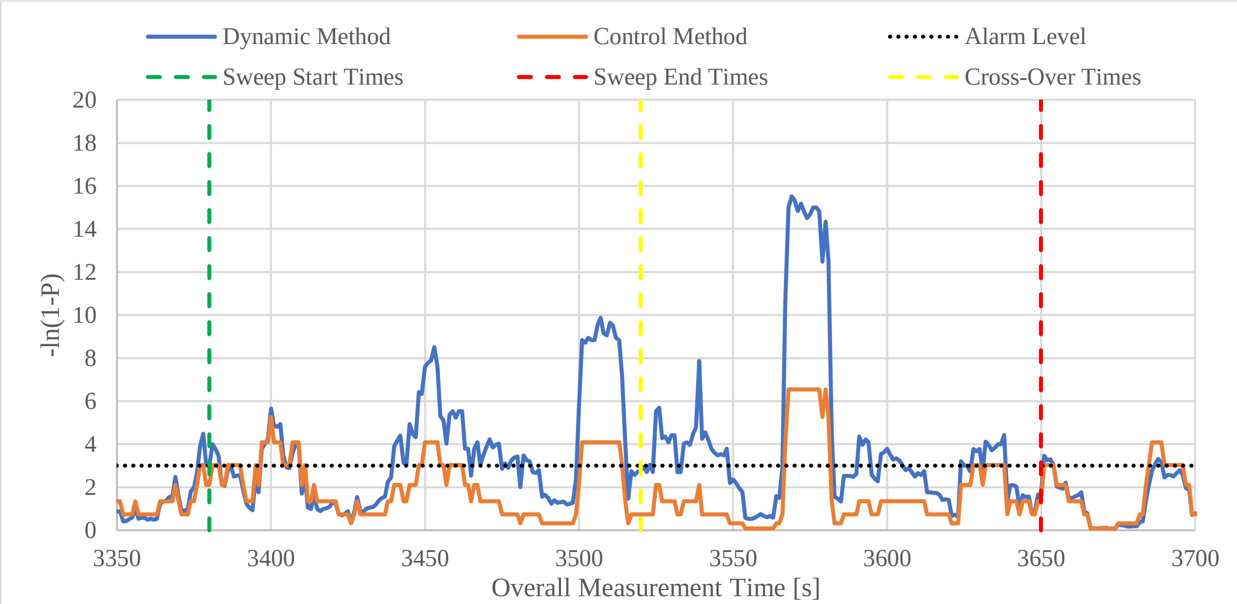

Figure 9. Alarm metrics over time during an MRSS sweep with the source on level 2. The sweep began and ended on level 8, as indicated by the green and red vertical dashed lines, respectively. The yellow vertical dashed line indicates the cross-over point from the downward section of the garage to the upward section on level 1. The dynamic method (blue) calculated the alarm metric using the predicted background neutron count rate, and the control method (orange) calculated the metric using the constant average background neutron count rate. An alarm would occur when these metrics' values were greater than the threshold indicated by the black dotted line.

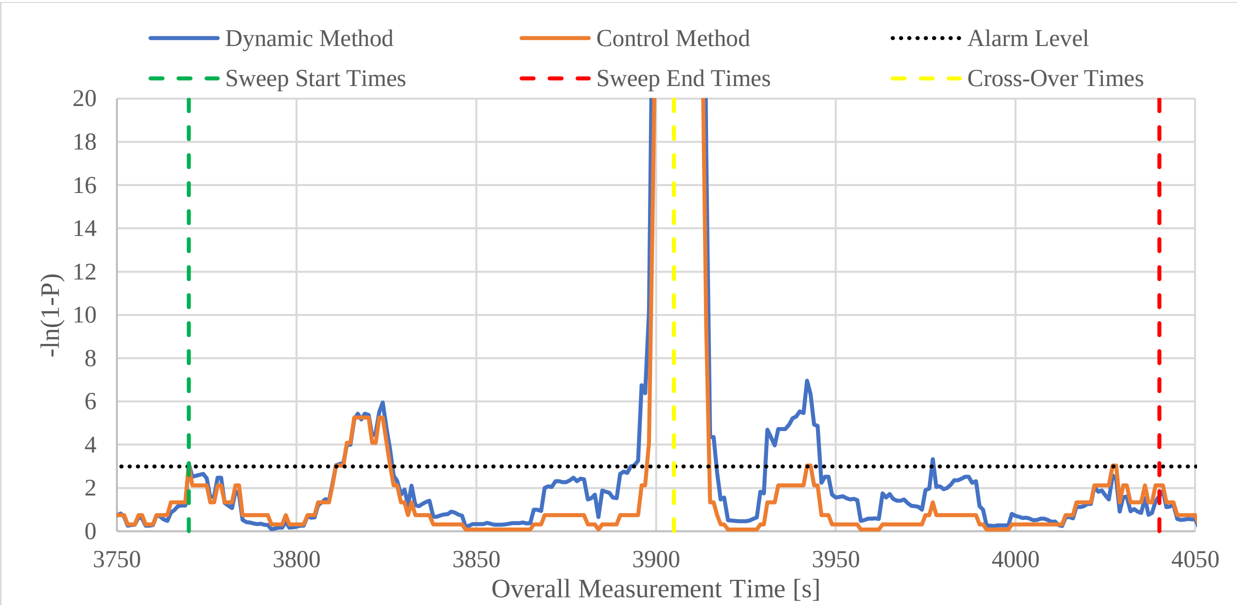

Figure 10. Alarm metrics over time during an MRSS sweep with the source on level 1. The sweep began and ended on level 8, as indicated by the green and red vertical dashed lines, respectively. The yellow vertical dashed line indicates the cross-over point from the downward section of the garage to the upward section on level 1. The dynamic method (blue) calculated the alarm metric using the predicted background neutron count rate, and the control method (orange) calculated the metric using the constant average background neutron count rate. An alarm would occur when these metrics' values were greater than the threshold indicated by the black dotted line.

DOI: 10.7290/ijns08497795

International Journal of Nuclear Security, Vol. 8, No. 1, 2023

As a comparison with these sweeps, the alarm metrics for the final background sweep over time are plotted in Figure 11. This figure shows that the alarm metrics did not increase as much as when the source was present, as expected. However, there were two instances where the dynamic alarm metric crossed the alarm threshold in a meaningful way. The two alarms' midpoints occurred at approximately 4300 and 4360 s, as shown in Figure 11, which would have been when the MRSS was on level 1 (the cross-over point) and level 3, respectively. One explanation for this result might be that although the source was not in the garage during this sweep, it was nearby; it was being secured in a building across the street during the first half of that sweep. These data suggest that the system was still observing excess neutrons from that source, albeit in a reduced fashion from the other tests, which the dynamic alarm metric was able to recognize as such. This result is further indicated by the fact that these alarms occurred when the MRSS was on or just above or below the ground level, where the garage walls would have had less of a shielding effect on that source than when the MRSS was at higher levels.

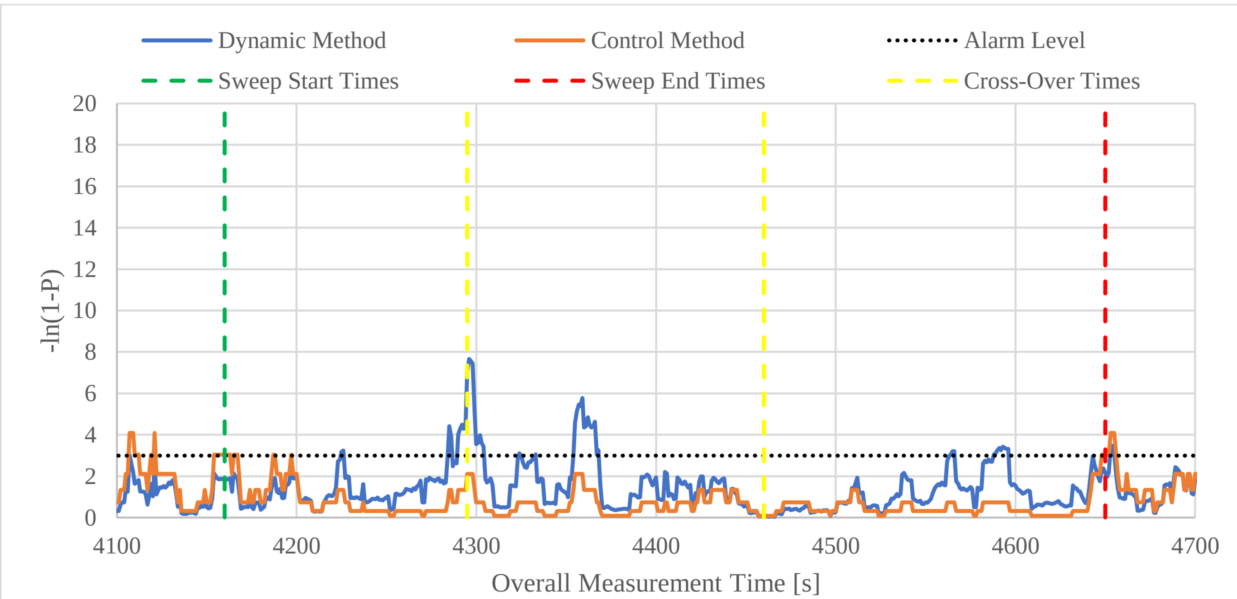

Figure 11. Alarm metrics over time during an MRSS sweep with no source in the garage. This experiment consisted of one full sweep starting from level 8 (green vertical dashed line) with an additional half-sweep that returned to level 1 to exit the garage (red vertical dashed line). The yellow vertical dashed lines indicate the cross-over points, with the first being from the downward section of the garage to the upward section at level 1 and the second being from the upward section to the downward section at level 8. The dynamic method (blue) calculated the alarm metric using the predicted background neutron count rate, and the control method (orange) calculated the metric using the constant average background neutron count rate. An alarm would occur when these metrics' values were greater than the threshold indicated by the black dotted line.

Similar to the background sweep, the alarm metrics under more normal background conditions (before the system entered the garage) are shown in Figure 12. These data were collected in a suburban-type environment, where few buildings were near the system but not in such a way that would affect the neutron or muon count rates. The source was brought in proximity to the detectors during the final setup, which caused

DOI: 10.7290/ijns08497795

the extremely high values between times 750 and 880 s. The system then entered the garage shortly after that (at 900 s) to get into position for the first sweep, thus producing the variable alarm metrics shown between 880 and 1050 s. These data, particularly those before 750 s, show that in less extreme environments (i.e., not in urban areas or a parking garage), both alarm metrics would produce similar values regardless of whether a neutron source is present.

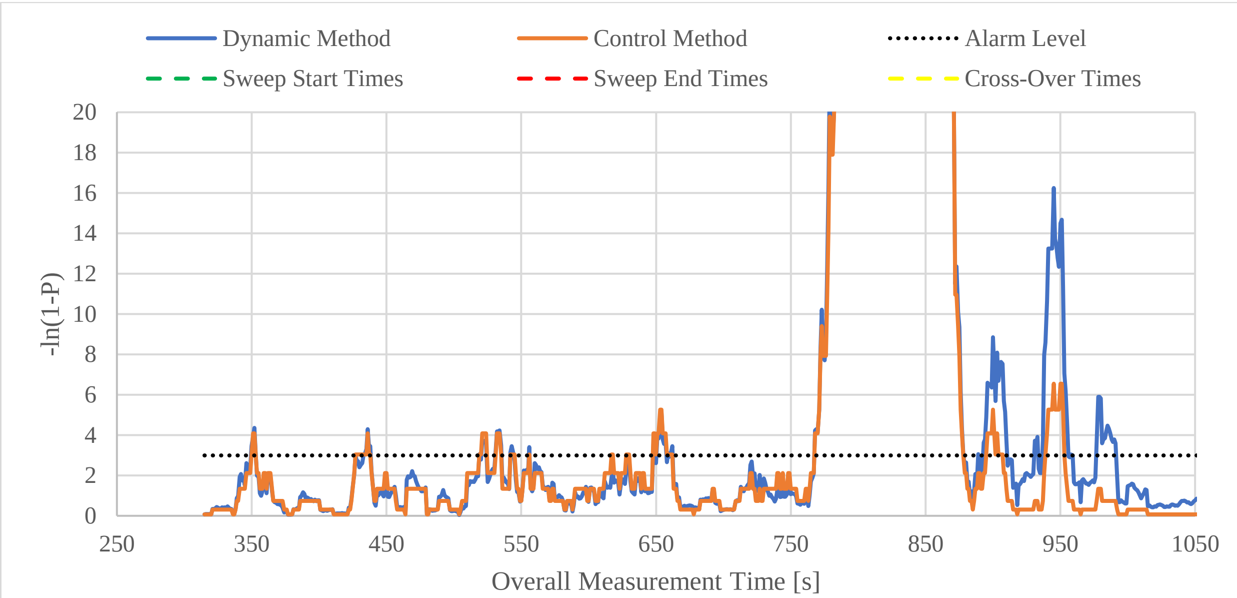

Figure 12. Alarm metrics over time prior to and just after entering the garage. The dynamic method (blue) calculated the alarm metric using the predicted background neutron count rate, and the control method (orange) calculated the metric using the constant average background neutron count rate (orange). Data from 300 to 700 s were used to calculate the average background neutron count rate used for the control method. The source was next to the system between 750 and 880 s. With the source in the garage, the system entered the garage at 900 s and moved into position for the first sweep after 1050 s.

One potential limitation for this method lies in the way a system measures the muon count rate. For these measurements, the muon count rate was the total counts between 4 and 70 MeV in a NaI detector. Measurements with this and similar systems have shown that the potential exists for excess detections at the lower end of this range. This occurred during a similar test with the previously described system, where the source was placed on the trunk of the vehicle (above the neutron detector). A plot of the relevant count rates during this time are shown in Figure 13. Those data show that the source caused the neutron count rate to increase significantly, but the muon count rate also increased, which in turn caused an increase in the estimated neutron count rate. However, Figure 14 shows that something similar did not occur when the source was nearby the mobile search system before it entered the parking garage.

International Journal of Nuclear Security, Vol. 8, No. 1, 2023

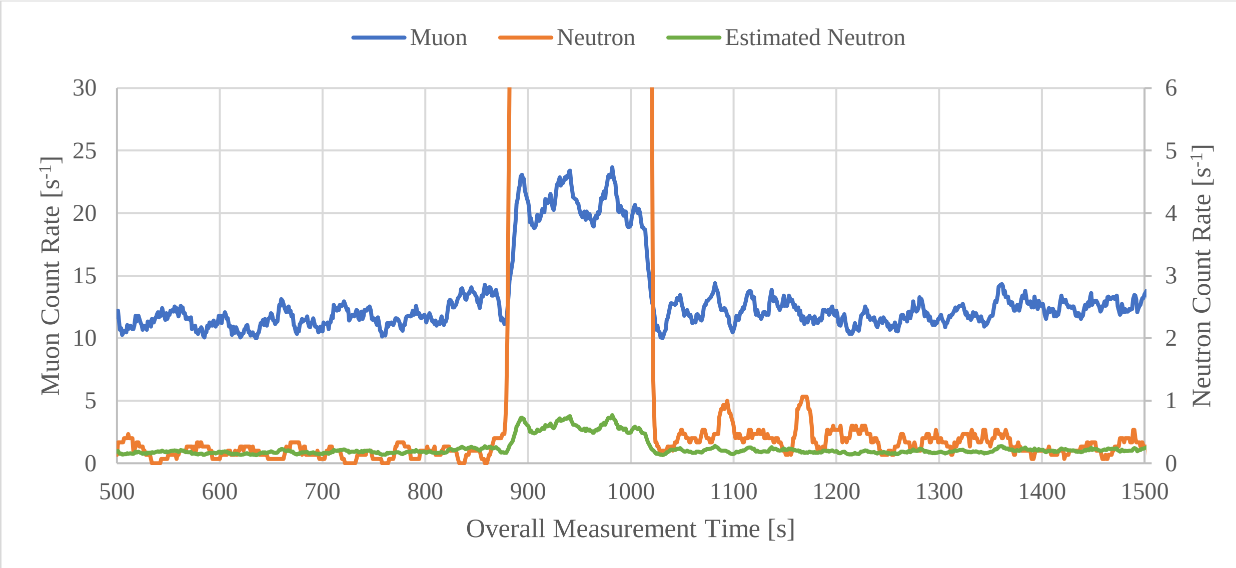

Figure 13. Muon (blue, left axis), observed neutron (orange, right axis), and estimated neutron (green, right axis) count rates over time during separate measurements with the mobile search system. The ^{252}Cf source was placed on the trunk of the mobile search vehicle between 870 and 1040 s.

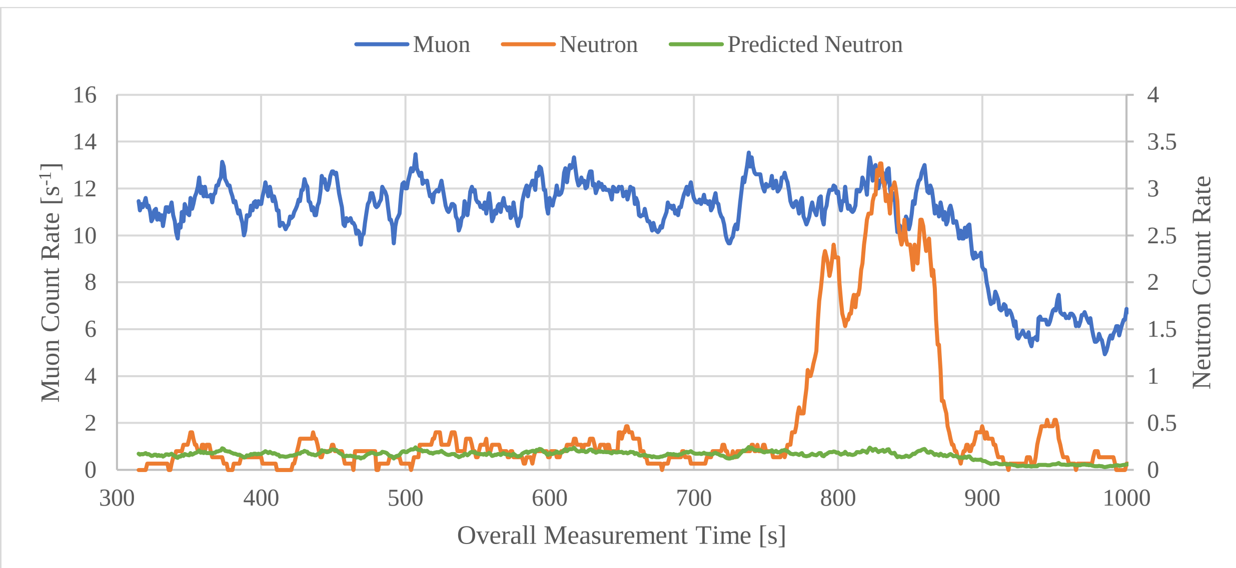

Figure 14. Muon (blue, left axis), observed neutron (orange, right axis), and estimated neutron (green, right axis) count rates over time before parking garage measurements with the mobile search system. The ^{252}Cf source was placed adjacent to the system between 750 and 880 s.

A similar phenomenon occurred during measurements performed by a US Department of Energy Radiological Assistance Program (RAP) team; these measurements were analyzed with previous work [3]. In that system, the muon count rate was the total counts in the NaI detector's overflow channel, which included counts between 3 MeV and approximately 12 MeV. During the measurements, the system was near an ion beam facility while it was active, which greatly increased their systems' neutron count rate, as seen in Figure 15. Similar to the data in Figure 13, there was also an increase

DOI: 10.7290/ijns08497795

in their overflow channel count rate, which caused the estimated neutron count rate to increase.

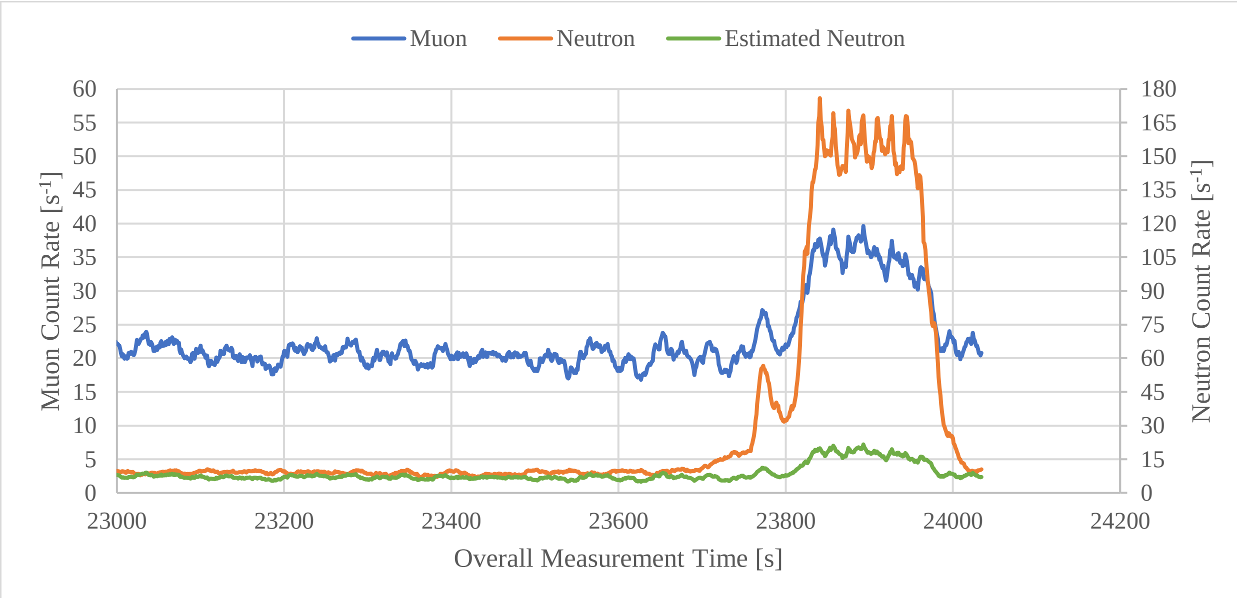

Figure 15. Muon (blue, left axis), observed neutron (orange, right axis), and estimated neutron (green, right axis) count rates over time during RAP measurements as part of previous work [3]. The ion beam facility was active between 23,700 and 24,000 s.

In both cases, the observed neutron count rate increased significantly to where an alarm still would have occurred despite the estimate being affected. Because of this, it is likely that the detections that occurred were the result of the sources themselves or secondary reactions they caused. In the case of the ^{252}Cf source, it is likely that the excess NaI detections were a result of (n, γ) reactions with materials in the vehicle. In this case, the ^{56}Fe(n, γ)^{57}Fe reaction is likely to occur in the vehicle's steel, and that reaction has a nontrivial probability of emitting gamma rays with energies up to 7.6 MeV [7]. This specific interaction is likely because the effect occurred when the source was placed on the vehicle (Figure 13) but not when the source was nearby for a significant period (Figure 14). Similar reactions are likely to have occurred in the scenario of the ion beam facility because of the excess radiation it may emit while active. However, the characteristics of that radiation and the nearby materials are unknown, which prevents any further speculation. These data suggest that it is plausible that such an effect may only occur with strong neutron sources, but more research would be required to confirm such a characteristic. This confirmation would be important because these appear to be the only scenarios where nonbackground environments would affect the estimate of the background neutron count rate.

4. Conclusion

This work shows that a dynamic estimate of the background neutron count rate from its power law relationship with an MRSS's muon count rate is a meaningful basis for a neutron alarm metric. Measurements of a source in a parking garage showed that the dynamic alarm method produced an alarm at the same rate or more often than a commonly used method that applies a constant estimate of the neutron background. A dynamic method such as this has the added benefit of being able to account for common background changes that an MRSS may observe, which should reduce an MRSS's false alarm rate. Also, it is conceivable that an improved estimate of the neutron background throughout an MRSS's operation would improve its sensitivity to neutron-emitting radiological materials (making it able to alert operators to smaller amounts). These aspects will require further study to quantify the potential reduction in an MRSS's false alarm rate and its minimum detectable activity.

5. Acknowledgments

The authors wish to thank Kevin G. Hart of Sandia National Laboratories and of the US Department of Energy's Radiological Assistance Program for providing portions of the data analyzed for this work.

6. References

1. Wagner, J. N.; Marianno, C. Identification of the Ambient Response Relationship in Neutron Counting and Scintillation Measurement Systems. *Radiation Science and Technology* **2021**, *7* (1), 7–14. DOI: 10.11648/j.rst.20210701.12.
2. Ziegler, J. F. Terrestrial Cosmic Rays. *IBM Journal of Research and Development* **1996**. DOI: 10.1147/rd.401.0019.
3. Wagner, J. N.; Marianno, C.; Cline, D. Characterization of a Gamma Spectrometer–Neutron Counter Background Correlation in Mobile Radiological Search Systems. *Nuclear Instruments and Methods in Physics Research Section A: Accelerators, Spectrometers, Detectors and Associated Equipment* **2021**, *1014*. DOI: 10.1016/j.nima.2021.165648.
4. Upp, D. L.; Keyser, R. M. Performance of a Car-Mounted Neutron and Gamma-Ray Monitoring System for Illicit Material Detection. In *Proc. 45th INMM Annual Meeting Institute of Nuclear Materials Management*, Institute of Nuclear Materials Management: 2004.
5. AMETEK Inc.—ORTEC. digiBASE 14-Pin PNT Tube Base with Integrated Bias Supply, Preamplifier, and MCA (with Digital Signal Processing) for NaI Spectroscopy. https://www.ortec-online.com/-/media/ametekortec/brochures/d/digibase.pdf?la=en&revision=de3aa261-0aa3-4f7c-9e01-68b134f29a11 (accessed 12-16-2023).
6. International Atomic Energy Agency. *IAEA Safeguards Glossary*; International Nuclear Verification Series No. 3; IAEA: Vienna, 2003.
7. Firestone, R. B.; et. al. Thermal Neutron Capture Cross Section for $^{56}Fe(n,\gamma)$. *Physical Review C* **2017**, *95* (014328). DOI: 10.1103/PhysRevC.95.014328.

DOI: 10.7290/ijns08497795